J. KSIAM Vol.8, No.2, 51-73, 2004

Hall and Ion-Slip effects on magneto-micropolar fluid with combined forced and free convection in boundary layer flow over a horizontal plate

M. A. Seddeek* and M. S. Abdelmeguid**

Abstract

A boundary layer analysis is used to study the effects of Hall and ion-slip currents on the steady magneto-micropolar of a viscous incompressible and electrically conducting fluid over a horizontal plate. By means of similarity solutions, deviation of fundamental equations on the assumption of small magnetic Reynolds number are solved numerically by using the shooting method. The effects of various parameters of the problem, e.g. the magnetic parameter, Hall parameter, ion-slip parameter, buoyancy parameter and material parameter are discussed and shown graphically.

1. Introduction

Eringen [1] formulated the theory of microploar fluids, which included the effects of local rotary inertia and couple stresses. These fluids are able to describe the behavior of colloidal solutions, suspension solutions, liquid crystal, animal blood, etc. The study of magneto-micropolar fluid flows in a slip-flow regime with Hall and ion-slip currents has attracted the interest of any investigators in view of its important applications in many engineering problems such as power generators, magnetohydrodynamic (MHD) accelerators, refrigeration coils, transmission lines, electric transformers and heating elements. The present problem finds application in MHD generators with neutral fluid seeding in the form of rigid microinclusions. Also, many industrial applications involve fluids as a working medium and in such applications unclean fluids (i.e., clean fluid + interspersed particles) are the rule and clean fluids an exception.

Mori [2] and Sparrow and Minkowycz [3] were the first investigators to treat the problem of combined convective heat transfer over a horizontal flat plate with the effects of buoyancy forces. Balaram and Sastry [4] and Maiti [5] studied the convection heat transfer in a micropolar fluid through a vertical channel and through a horizontal parallel plate channel. The free convection in the boundary layer flow of a micropolar fluid past a non-isothermal vertical flat plate has been studied by Jena and Mathur [6]. Hassanien [7] studied

2000 Mathematics Subject Classification : 76R10

the steady mixed convection in micropolar boundary layer flow on a horizontal plate.

The effects of Hall and ion-slip currents in steady MHD free convective flow past an infinite vertical porous plate in a rotating frame of reference when the heat flux is maintained as constant at the plate was studied by Ram [8]. Later, Ram and Takhar [9] dealt with MHD free convection from an impulsively moving infinite vertical plate in a rotating fluid with Hall and ion-slip currents. Pop and Watanable [10] studied the effects of Hall current on MHD free convection flow past a semi-infinite vertical flat plate. The effects of Hall and ion-slip currents on free convective heat generating flow in a rotating fluid were analysed by Ram [11]. Kinyanjui et al. [12] studied the effects of Hall current in the MHD Stokes problem for a vertical infinite plate in a rotating fluid. Seddeek [13] studied the effects of Hall and ion-slip currents on magneto-micropolar fluid and heat transfer over a non- isothermal stretching sheet with suction and blowing. Recently, Seddeek [14] studied the flow of a micropolar fluid past a moving plate by the presence of magnetic field.

In the present work, the aim is to investigate the Hall and ion-slip current effects of neutral seeding of the fluid, in the form of introducing relatively rigid microelements in the fluid which is moving in the presence of a magnetic field. A linear micropolar fluid as presented by Eringen [1] is assumed to represent the model of the fluid under consideration. We have chosen to call the fluid under discussion a magneto-micropolar fluid. The criteria for Hall and ion-slip current effects on magneto-micropolar fluid with boundary layer mixed convection flow over a horizontal plate are then obtained. Numerical results are presented for range of values of Hall parameter, ion-slip parameter, magnetic parameter, material parameter and buoyancy parameter of the fluid.

2. Mathematical Analysis

Consider a steady laminar, incompressible, viscous, electrically conducting fluid flowing past a semi-infinite horizontal plate having a uniform free stream velocity U_∞, density ρ_∞ and temperature T_∞. The x-axis is assumed to be taken along the plate and the y-axis normal to the plate. A transverse strong magnetic field B_0 with constant intensity is imposed along the y-axis. For an electrically conducting fluid, the Hall and ion-slip currents significantly affect the flow in the presence of large magnetic field. The induced magnetic field is neglected, since the magnetic Reynolds number is assumed to be very small (Shercliff [15]). The effects of Hall current gives rise to a force in the z-direction, which induces a cross flow in that direction, and hence, the flow becomes three-dimensional. We assume that there is no variation of flow or heat transfer quantities in the z-direction. The governing boundary layer equations may be written as

$$\frac{\partial u}{\partial x}+\frac{\partial v}{\partial y}=0, \tag{1}$$

$$u\frac{\partial u}{\partial x} + v\frac{\partial u}{\partial y} = \left(\nu + \frac{k}{\rho_\infty}\right)\frac{\partial^2 u}{\partial y^2} - \frac{1}{\rho_\infty}\frac{\partial p}{\partial x} + \frac{k}{\rho_\infty}\frac{\partial N}{\partial y} - \frac{B_0}{\rho_\infty} j_z , \quad (2)$$

$$u\frac{\partial w}{\partial x} + v\frac{\partial w}{\partial y} = \left(\nu + \frac{k}{\rho_\infty}\right)\frac{\partial^2 w}{\partial y^2} + \frac{B_0}{\rho_\infty} j_x , \quad (3)$$

$$\frac{1}{\rho_\infty}\frac{\partial p}{\partial y} = g\,\beta_\infty\left(T - T_\infty\right), \quad (4)$$

$$u\frac{\partial N}{\partial x} + v\frac{\partial N}{\partial y} = \frac{\gamma}{\rho_\infty J^*}\frac{\partial^2 N}{\partial y^2} - \frac{K}{\rho_\infty J^*}\left(2N + \frac{\partial u}{\partial y}\right), \quad (5)$$

$$u\frac{\partial T}{\partial x} + v\frac{\partial T}{\partial y} = \frac{k_f}{\rho_\infty C_p}\frac{\partial^2 T}{\partial y^2} , \quad (6)$$

where u, v and w are the velocity components in the x, y and z directions, respectively; N is the angular velocity; T is the fluid temperature; ν, k and γ are the viscosity coefficients, J^* is the micro inertia per unit mass; k_f is the thermal conductivity; C_p is the specific heat at constant pressure, g is the gravitational constant and β_∞ is the coefficient of volumetric expansion.

The boundary conditions are given by

$$\begin{aligned} &y = 0 \;:\; u = v = w = 0 \;,\; N = 0 \;,\; T = T_w(x) \\ &y \to \infty \;:\; u \to U_\infty \;,\; N \to 0 \;,\; w \to 0 \;,\; T \to T_\infty \;,\; p \to p_\infty \end{aligned} \quad (7)$$

where p_∞ is the hydrostatic pressure in the undisturbed fluid.

The equation of conservation of electric charge $\nabla . \vec{J} = 0$ gives $j_y = \text{constant}$, where $\vec{J} = \left(j_x , j_y , j_z\right)$. This constant is assumed to be zero, since $j_y = 0$ everywhere in the flow. The expressions for the current density components j_x and j_z as obtained from the generalized Ohm's law (Sutton and Sherman [16]), are given by

$$j_x = \frac{\sigma}{\alpha_e^2 + \beta_e^2}\left[\alpha_e\left(E_x - w B_o\right) + \beta_e\left(E_z + u B_o\right)\right],$$

$$j_z = \frac{\sigma}{\alpha_e^2 + \beta_e^2}\left[\alpha_e\left(E_z + u B_o\right) - \beta_e\left(E_x - w B_o\right)\right].$$

Where β_e is the Hall parameter, β_i is the ion-slip parameter, σ is the electrical conductivity and $\alpha_e = 1 + \beta_i \beta_e$. In the absence of electric field $\left(E_x = E_z = 0\right)$, we get

$$j_x = \frac{\sigma B_o}{\alpha_e^2 + \beta_e^2}\left(\beta_e u - \alpha_e w\right), \tag{8}$$

$$j_z = \frac{\sigma B_o}{\alpha_e^2 + \beta_e^2}\left(\alpha_e u + \beta_e w\right). \tag{9}$$

Now, we use the dimensionless variable, which takes the form

$$X = \frac{x}{L}, \qquad Y = \sqrt{\frac{Re}{X}}\,\frac{y}{L};$$

$$U = \frac{u}{U_\infty}, \qquad V = \sqrt{\frac{Re}{X}}\,\frac{v}{U_\infty}, \qquad W = \frac{w}{U_\infty};$$

$$N_1 = \frac{N L}{U_\infty}\sqrt{\frac{X}{Re}}; \qquad \theta = \frac{T - T_\infty}{T^*}; \qquad P = \frac{p - p_\infty}{\rho_\infty U_\infty^2};$$

$$\lambda = \frac{\gamma}{\mu J^*}; \qquad B = \frac{\nu^2 Re}{J^* U_\infty^2}; \qquad Ar = \frac{g L \beta_\infty T^*}{U_\infty^2} \text{ (Archimedes number);}$$

$$Re = \frac{U_\infty x}{\nu} = \frac{U_\infty X L}{\nu} \text{ (Reynolds number);} \qquad \Delta = \frac{k}{\mu} \text{ (material parameter);}$$

$$\Omega = Ar\sqrt{\frac{X}{Re}} \text{ (Buoyancy parameter);} \qquad Pr = \frac{\rho_\infty \nu C_p}{k_f} \text{ (Prandtl number);}$$

$$M = \frac{\sigma \nu Re B_o^2}{\rho_\infty U_\infty^2} \text{ (Magnetic parameter),} \tag{10}$$

where T^* represents a characteristic temperature difference between plate and free stream and L is the value of the x-coordinate where $T^* = T_w - T_\infty$. λ and B are the micropolar fluid parameters.

We further define the following similarity variables,

$$\eta = Y X^{-\frac{1}{2}} \quad , \qquad \Psi = X^{\frac{1}{2}} f(\eta);$$

$$N_1 = X^{-\frac{1}{2}} g(\eta); \qquad \theta = X^{-\frac{1}{2}} \Phi(\eta); \qquad W = h(\eta). \tag{11}$$

With $U = \frac{\partial \Psi}{\partial Y}$, $V = -\frac{\partial \Psi}{\partial X}$ and introducing equations (8), (9), (10) and (11) into equations (2), (3), (5) and (6) give

$$2(1+\Delta)f''' + f f'' + 2\Delta g' + \Omega \eta \Phi - \frac{2M}{\alpha_e^2 + \beta_e^2}(\alpha_e f' + \beta_e h) = 0, \tag{12}$$

$$2(1+\Delta)h'' + f h' - \frac{2M}{\alpha_e^2 + \beta_e^2}(\alpha_e h - \beta_e f') = 0, \tag{13}$$

$$\lambda g'' + \frac{1}{2}(f' g + f g') - \Delta . B(2g + f'') = 0, \tag{14}$$

$$\frac{2}{Pr}\Phi'' + f \Phi' + f' \Phi = 0. \tag{15}$$

In the above equations, a prime denotes differentiation with respect to η only.
The transformed boundary conditions are given by:

$$f(0)=0 \ , \ f'(0)=0 \ , \ h(0)=0 \ , \ g(0)=0 \ , \ \Phi(0)=1,$$

$$f'(\infty)=1 \quad , \quad h(\infty)=0 \quad , \quad g(\infty)=0 \quad , \quad \Phi(\infty)=0 \tag{16}$$

3. Numerical results and discussion

Equations (12) – (15) with the boundary condition (16) have been solved by the shooting method. The double precision arithmetic was used in all computation. A step size of $\Delta\eta = 0.001$ was selected. The results obtained for steady flow are displayed in Tables 1 – 5 and Figures 1.1 – 9.2. for Pr = 0.7, $\lambda = 0.5$ and B = 0.01 at different values of the Hall parameter β_e, the ion-slip parameter β_i, the material parameter Δ, the magnetic field parameter M and the buoyancy parameter Ω.

Table 1. Results of $f''(0)$, $h'(0)$, $-g'(0)$ and $-\Phi'(0)$ with β_e ($\beta_i = 0.4$, $\Delta = 4.5$, $M = 0.3$ and $\Omega = 0.5$)

β_e	$f''(0)$	$h'(0)$	$-g'(0)$	$-\Phi'(0)$
0.4	0.257505	0.023449	0.058198	0.003569
0.8	0.274777	0.032818	0.059906	0.002785
1	0.282045	0.034352	0.060592	0.002511
2	0.304935	0.031479	0.062640	0.001818
4	0.320768	0.021502	0.063967	0.001458

Table 2. Results of $f''(0)$, $h'(0)$, $-g'(0)$ and $-\Phi'(0)$ with β_i ($\beta_e = 5$, $\Delta = 4.5$, $M = 0.3$ and $\Omega = 0.5$)

β_i	$f''(0)$	$h'(0)$	$-g'(0)$	$-\Phi'(0)$
0.1	0.327374	0.023139	0.064507	0.001329
0.5	0.323465	0.016607	0.064186	0.001405
1	0.323341	0.010125	0.064173	0.001408
3	0.328286	0.002246	0.064573	0.001314
5	0.330600	0.000910	0.064759	0.001272

Table 3. Results of $f''(0)$, $h'(0)$, $-g'(0)$ and $-\Phi'(0)$ with Δ ($\beta_e = 5$, $\beta_i = 0.4$, $M = 0.3$ and $\Omega = 0.5$)

Δ	$f''(0)$	$h'(0)$	$-g'(0)$	$-\Phi'(0)$
0.5	0.644486	0.060437	0.009779	0.000190
1.5	0.499981	0.039599	0.027546	0.000399
4.5	0.323993	0.018244	0.064230	0.001394
13.5	0.182764	0.006133	0.097973	0.004621

Table 4. Results of $f''(0)$, $h'(0)$, $-g'(0)$ and $-\Phi'(0)$ with M
($\beta_e = 5$, $\beta_i = 0.4$, $\Delta = 4.5$ and $\Omega = 0.5$)

M	$f''(0)$	$h'(0)$	$-g'(0)$	$-\Phi'(0)$
1	0.295611	0.054087	0.061859	0.002061
3	0.210767	0.111091	0.053500	0.006604
5	0.141519	0.122701	0.044469	0.017098

Table 5. Results of $f''(0)$, $h'(0)$, $-g'(0)$ and $-\Phi'(0)$ with Ω
($\beta_e = 5$, $\beta_i = 0.4$, $\Delta = 4.5$ and M = 0.3)

Ω	$f''(0)$	$h'(0)$	$-g'(0)$	$-\Phi'(0)$
0	0.127679	0.011909	0.046599	0.012969
0.1	0.178133	0.013799	0.052414	0.006988
0.3	0.258423	0.016398	0.059610	0.002787
0.5	0.323993	0.018244	0.064230	0.001394
1	0.456726	0.021446	0.071409	0.000393

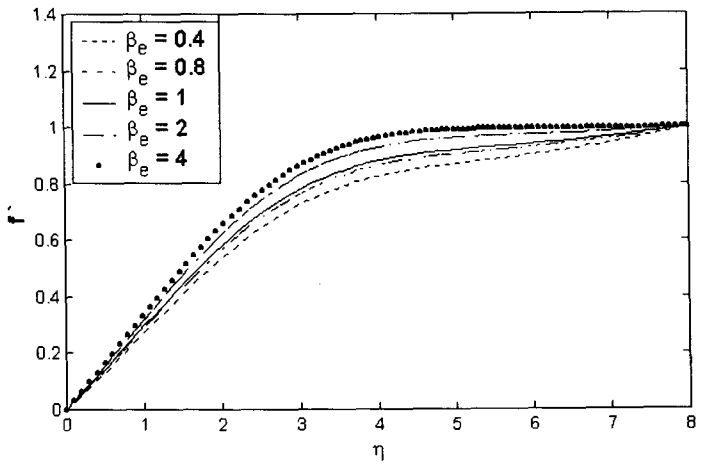

Figure 1.1. Distribution of velocity profiles along the plate at $\beta_i = 0.4$, $\Delta = 4.5$, M = 0.3 and $\Omega = 0.5$.

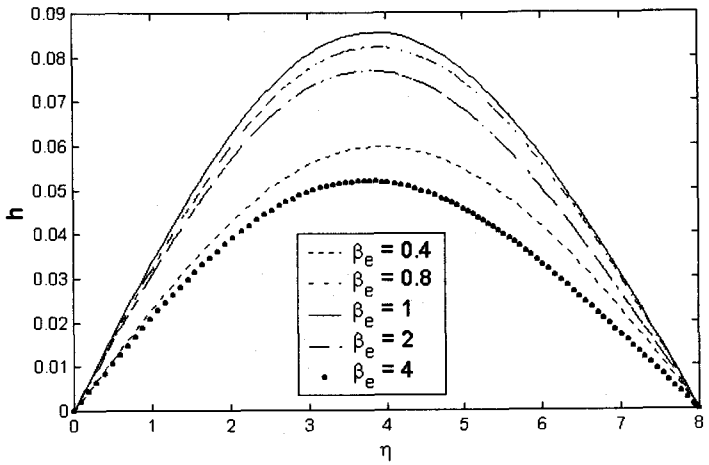

Figure 1.2. Distribution of velocity profiles across the plate at $\beta_i = 0.4$, $\Delta = 4.5$, $M = 0.3$ and $\Omega = 0.5$.

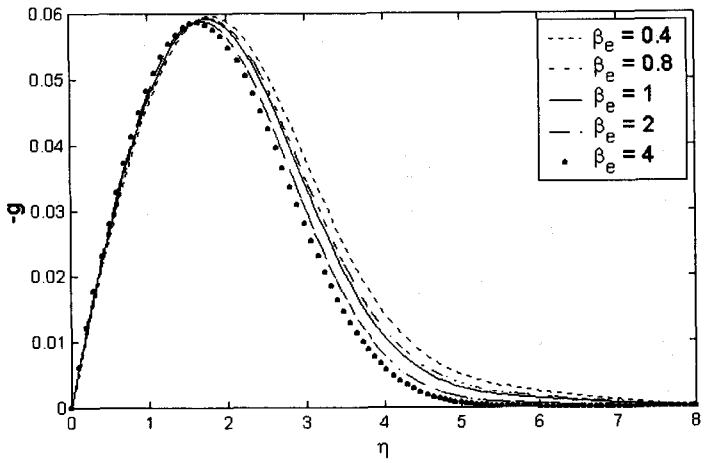

Figure 1.3. Distribution of angular velocity profiles at $\beta_i = 0.4$, $\Delta = 4.5$, $M = 0.3$ and $\Omega = 0.5$.

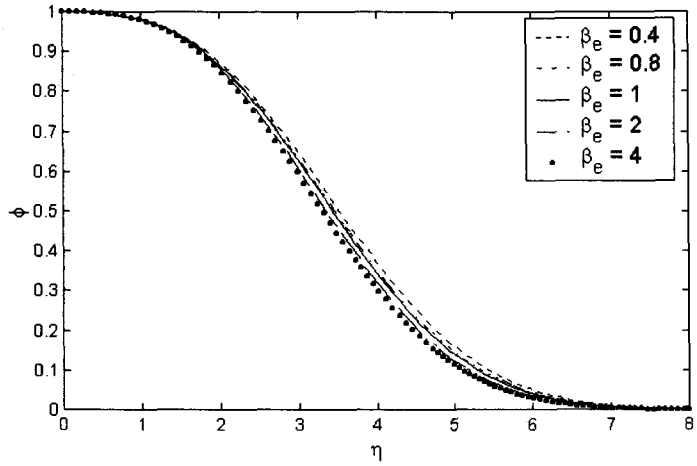

Figure 1.4. Distribution of temperature profiles at $\beta_i = 0.4$, $\Delta = 4.5$, $M = 0.3$ and $\Omega = 0.5$.

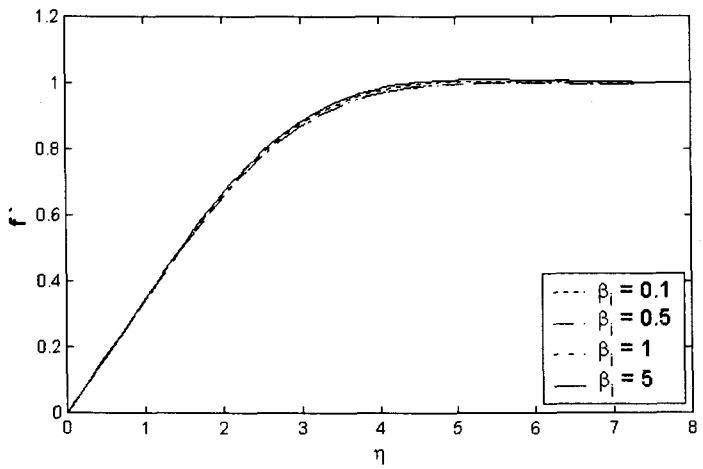

Figure 2.1. Distribution of velocity profiles along the plate at $\beta_e = 5$, $\Delta = 4.5$, $M = 0.3$ and $\Omega = 0.5$.

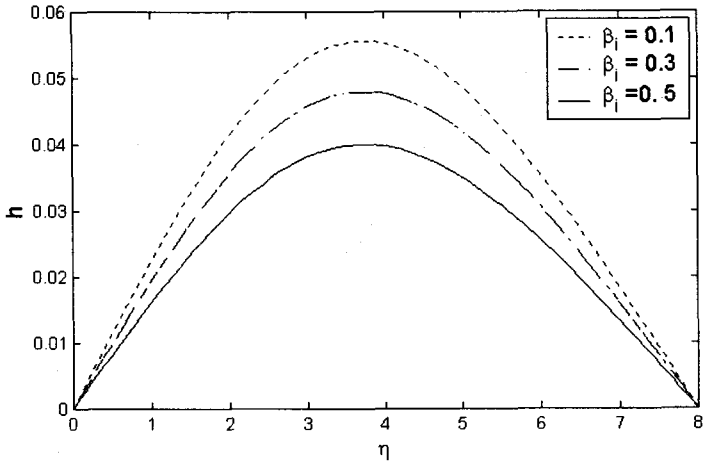

Figure 2.2. Distribution of velocity profiles across the plate at $\beta_e = 5$, $\Delta = 4.5$, $M = 0.3$ and $\Omega = 0.5$.

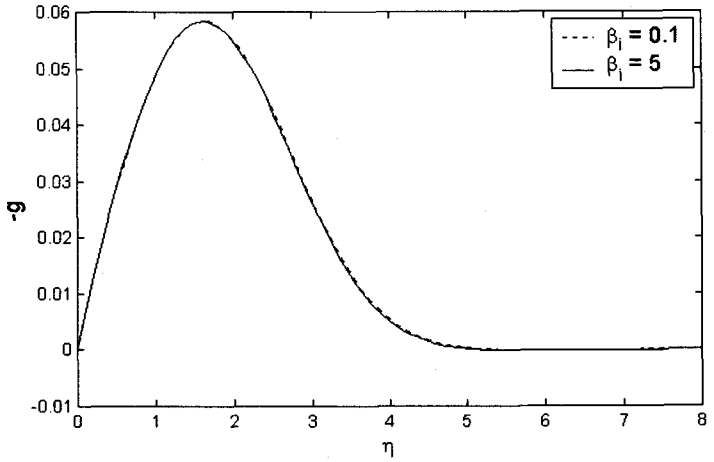

Figure 2.3. Distribution of angular velocity profiles at $\beta_e = 5$, $\Delta = 4.5$, $M = 0.3$ and $\Omega = 0.5$.

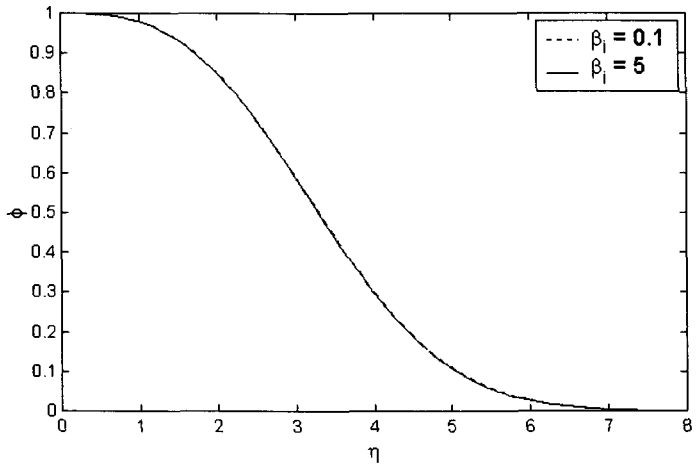

Figure 2.4. Distribution of temperature profiles at $\beta_e = 5$, $\Delta = 4.5$, $M = 0.3$ and $\Omega = 0.5$.

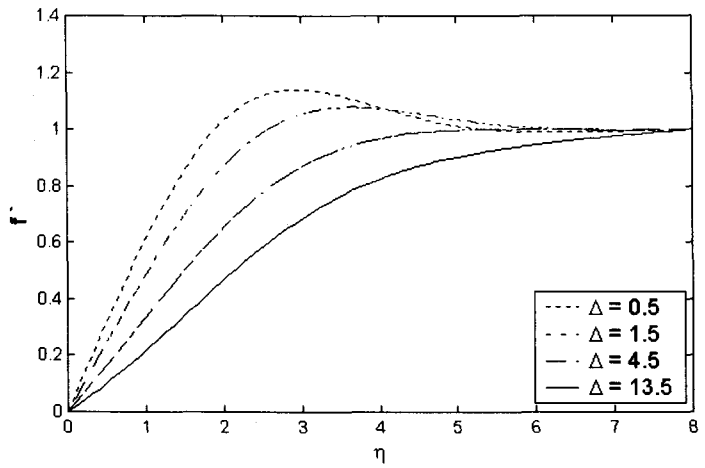

Figure 3.1. Distribution of velocity profiles along the plate at $\beta_e = 5$, $\beta_i = 0.4$, $M = 0.3$ and $\Omega = 0.5$.

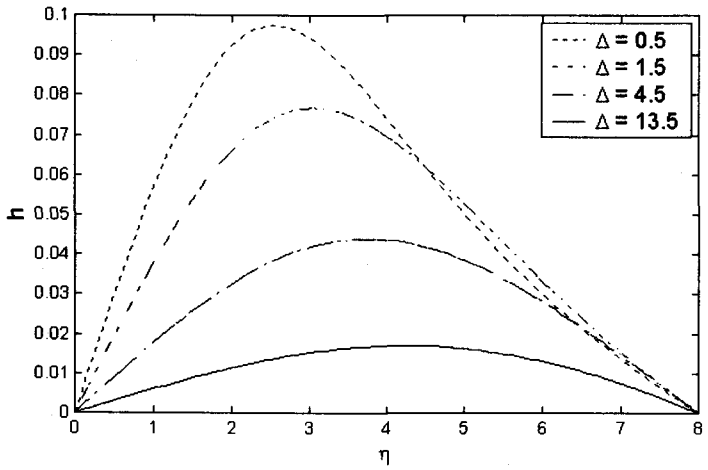

Figure 3.2. Distribution of velocity profiles across the plate at $\beta_e = 5$, $\beta_i = 0.4$, $M = 0.3$ and $\Omega = 0.5$.

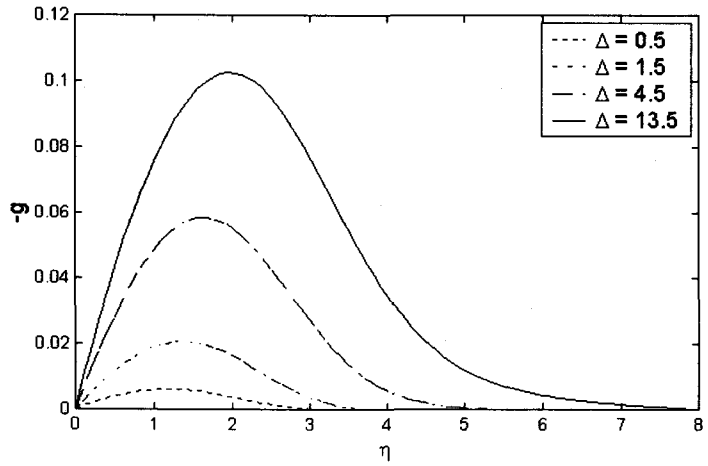

Figure 3.3. Distribution of angular velocity profiles at $\beta_e = 5$, $\beta_i = 0.4$, $M = 0.3$ and $\Omega = 0.5$.

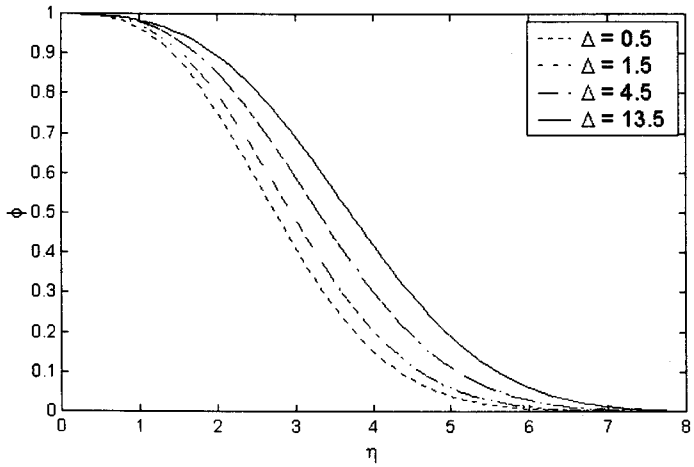

Figure 3.4. Distribution of temperature profiles at $\beta_e = 5$, $\beta_i = 0.4$, $M = 0.3$ and $\Omega = 0.5$.

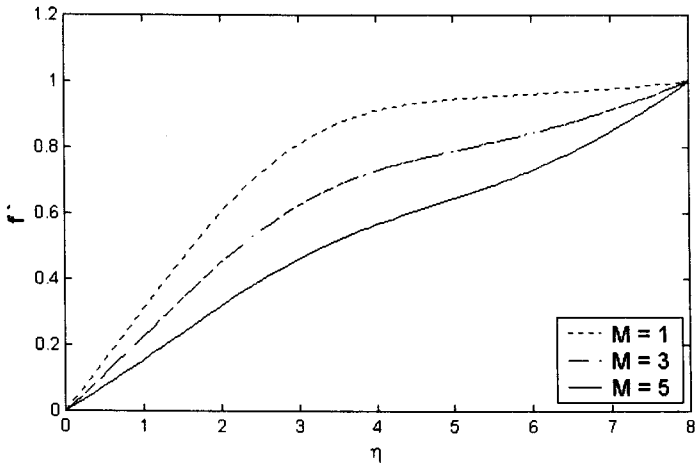

Figure 4.1. Distribution of velocity profiles along the plate at $\beta_e = 5$, $\beta_i = 0.4$, $\Delta = 4.5$ and $\Omega = 0.5$.

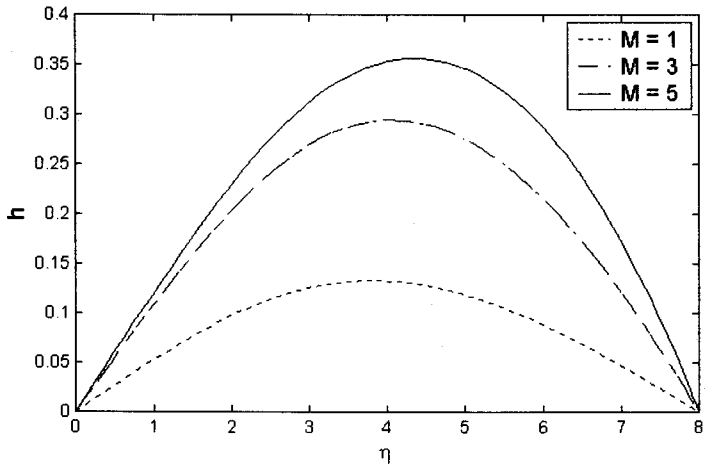

Figure 4.2. Distribution of velocity profiles across the plate at $\beta_e = 5$, $\beta_i = 0.4$, $\Delta = 4.5$ and $\Omega = 0.5$.

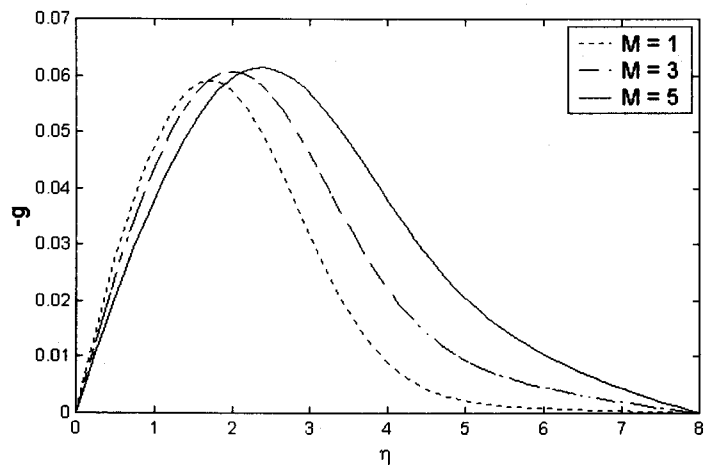

Figure 4.3. Distribution of angular velocity profiles at $\beta_e = 5$, $\beta_i = 0.4$, $\Delta = 4.5$ and $\Omega = 0.5$.

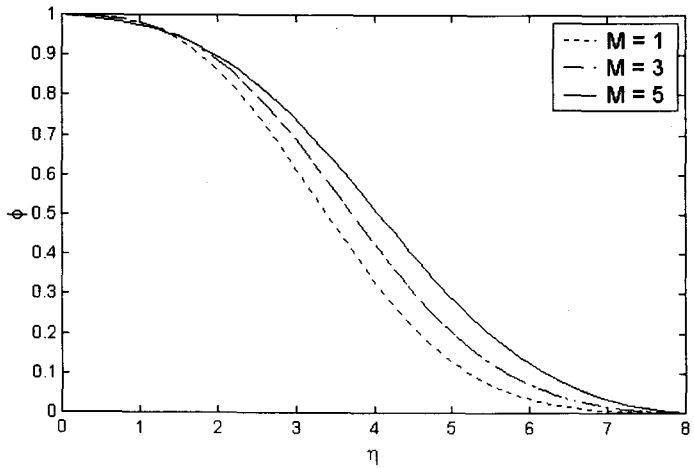

Figure 4.4. Distribution of temperature profiles at $\beta_e = 5$, $\beta_i = 0.4$, $\Delta = 4.5$ and $\Omega = 0.5$.

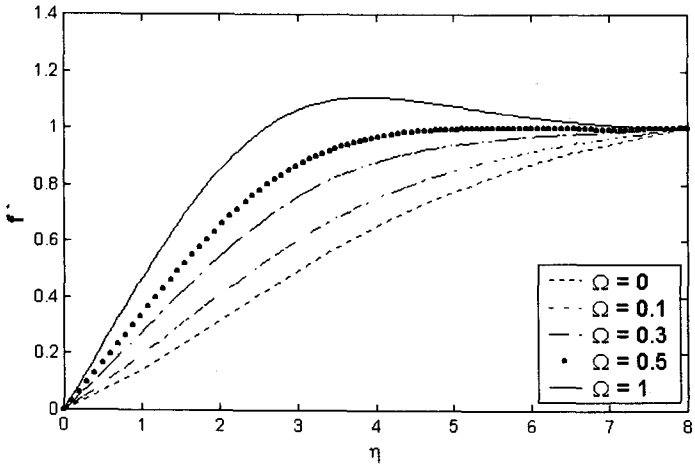

Figure 5.1. Distribution of velocity profiles along the plate at $\beta_e = 5$, $\beta_i = 0.4$, $\Delta = 4.5$ and M = 0.3.

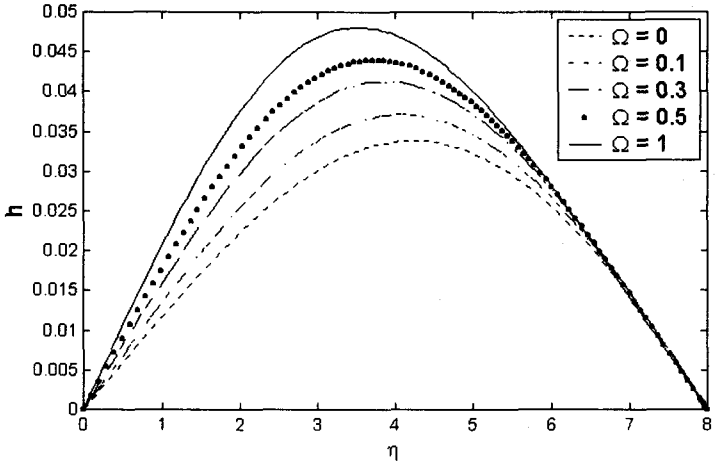

Figure 5.2. Distribution of velocity profiles across the plate at $\beta_e = 5$, $\beta_i = 0.4$, $\Delta = 4.5$ and $M = 0.3$.

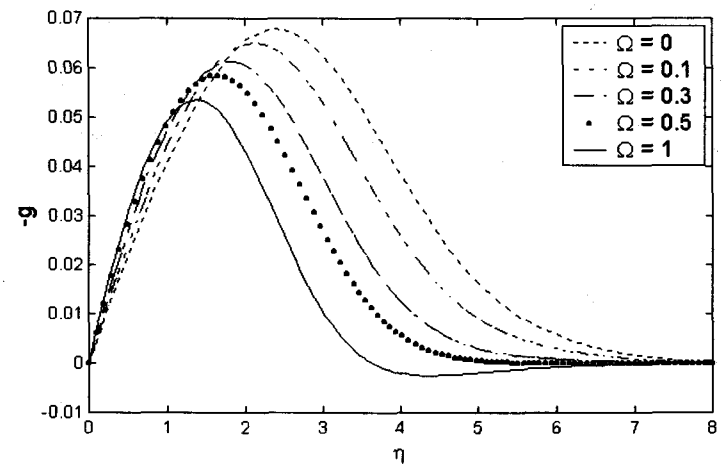

Figure 5.3. Distribution of angular velocity profiles at $\beta_e = 5$, $\beta_i = 0.4$, $\Delta = 4.5$ and $M = 0.3$.

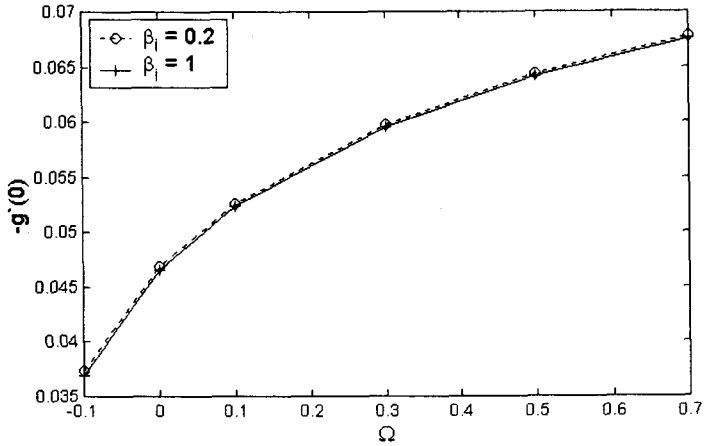

Figure 9.2. Dimensionless wall couple stress $-g'(0)$ as a function of the buoyancy parameter Ω for various ion-slip parameter β_i ($\beta_e = 5$, $\Delta = 4.5$ and $M = 0.3$).

It's seen from Figures1.1-1.4. that, the variation of distribution of velocity $f'(\eta)$, velocity across the plate $h(\eta)$, angular velocity $g(\eta)$ and temperature $\Phi(\eta)$ for several values of β_e. We see that the dimensionless velocity component $f'(\eta)$ and the angular velocity $g(\eta)$ increase with increasing parameter β_e. Figure 1.2. shows that the induced flow in the z-direction begins to develop as β_e increases in the interval $0 \leq \beta_e \leq 1$ and decreases for $\beta_e > 1$.

Figures 2.1.-2.4. represent the effect of the ion-slip parameter β_i on $f'(\eta)$, $h(\eta)$, $g(\eta)$ and $\Phi(\eta)$. It can be seen from these figures that the velocity $f'(\eta)$ and the angular velocity $g(\eta)$ decrease slowly with increasing parameter β_i in the interval $0 \leq \beta_i \leq 1$ and increase slowly for $\beta_i > 1$. The induced flow in the z-direction decreases with increasing the parameter β_i. As the ion-slip parameter β_i increases, the temperature distributions $\Phi(\eta)$ decreases more slowly.

Figures 3.1.-3.4. display the effect of the material parameter Δ on $f'(\eta)$, $h(\eta)$, $g(\eta)$ and $\Phi(\eta)$ within the boundary layer. It can be seen from these figures that the magnitudes of the velocity of micropolar fluid are smaller than that of Newtonian fluids. This is attributed to the fact that the increased viscosity of the micropolar fluid reduces its

velocity. As the material parameter Δ increases, the induced flow in the z-direction and the temperature distribution decrease. It is also clear from these figures that, as the material parameter Δ increases, the magnitudes of the maximum values of the angular velocity increase and the inflection point for the angular velocity distribution moves further away from the surface.

Figure 4.1.-4.4. describe the behavior of $f'(\eta)$, $h(\eta)$, $g(\eta)$ and $\Phi(\eta)$ for different values of the magnetic field parameter M. The dimensionless velocity component $f'(\eta)$ decreases with an increase in M. It is not surprising to have the result, sine the magnetic field exerts a retarding force on the free convection flow and because of an accelerating force, which acts in a direction parallel to the x-axis when Hall and ion-slip currents are absent. As the magnetic parameter M increases, the angular velocity $g(\eta)$ and the temperature distributions $\Phi(\eta)$ decrease. The induced flow in the z-direction increases with increasing in M.

Figure 5.1.-5.4. indicate the effect of the buoyancy parameter Ω on $f'(\eta)$, $h(\eta)$, $g(\eta)$ and $\Phi(\eta)$. As the buoyancy parameter Ω increases, the velocity distribution, the induced flow in the z-direction and the angular velocity increase. It is also clear that the temperature profile $\Phi(\eta)$ increases with an increase in Ω.

Results for the local wall shear stress and wall couple stress are presented against the buoyancy parameter in Figures from 6.1. until 9.2. for both the Newtonian and micropolar fluids. The results indicate that, for positive values of Ω (i.e., plate temperature larger than free-stream temperature) there is a favorable pressure gradient above the plate due to the buoyancy effects. The wall shear stress and wall couple stress are larger than that of the non-buoyant case. For negative values of Ω (i.e., the plate temperature is smaller than free-stream temperature), the opposite is true. Tables from1 until 5 present the results for $f''(0)$, $h'(0)$, $-g'(0)$ and $-\Phi'(0)$ at different values of β_e, β_i, Δ, M and Ω.

Finally, we observe that, the presence of microelements is found to be an important application in the control of flow separation. In comparison to the results for Newtonian fluids, it is noticed that micropolar fluids display both drag reduction and heat transfer rate reduction. Also, we notice from our results of the present study that unclean fluids may, in fact, be preferable to clean fluids in applications where control of convection is important.

References

[1] A. C. Eringen, J. Math. Mech. 16 (1966), 1.
[2] J. Mori, J. Heat Transfer ASME, Series C 83 (1961), 479.
[3] E. M. Sparrow and W. J. Minkowycz, Int. J. Heat Mass Transfer 5 (1962), 505.
[4] M. Balaram and V. U. K. Sastry, Int. J. Heat Mass Transfer 16 (1973), 437.
[5] G. Maiti, ZAMM 55 (1975), 105.
[6] S. K. Jena and M. N. Mathur, Int. J. Engng. Sci. 19 (1981), 1431.

[7] I. A. Hassanien, Z.angew. Math. Phys. 48 (1997), 571.
[8] P. C. Ram, Warme-und Stoffubertragung, 26 (1991), 203.
[9] P. C. Ram and H. S. Takhar, Fluid Dynamics Res., 11 (1993), 99.
[10] I. Pop and T. Watanabe, Int. J. Engng Sci. 32 (1994), 1903.
[11] P. C. Ram, Int. J. Energy Research, 19 (1995), 371.
[12]M. Kinyanjui, N. Chaturvedi and S. M. Uppal, Energy Conversion Mgmt., 39(5/6), (1998), 541.
[13] M. A. Seddeek, Proc. R. Soc. London A 457 (2001), 3039.
[14] M. A. Seddeek, Physics Letters A 306 (2003), 255.
[15] J. A. Shercliff, A textbook of magnetohydrodynamics, Pergamon Press, New York, USA (1965).
[16] G. W. Sutton and A. Sherman, Engineering magnethydrodynamics. New York : McGraw-Hill (1965).

*Department of mathematics, Faculty of Science
Helwan University, Ain Helwan, 11795, Cairo, Egypt.

** Akhbar EL-Yom Academy, 6 October City, Giza 12573, Egypt.